J|A|C|S
ARTICLES
Published on Web 04/27/2004

Solvent-Induced Self-Assembly of Mixed Poly(methyl methacrylate)/Polystyrene Brushes on Planar Silica Substrates: Molecular Weight Effect

Bin Zhao,*,† Richard T. Haasch,‡ and Scott MacLaren‡

Contribution from the Department of Chemistry, University of Tennessee at Knoxville, Knoxville, Tennessee 37996, and Materials Research Laboratory, University of Illinois, Urbana, Illinois 61801

Received January 24, 2004; E-mail: zhao@novell.chem.utk.edu

Abstract: The effect of molecular weight on the solvent-induced self-assembly of mixed poly(methyl methacrylate) (PMMA)/polystyrene (PS) brushes on silicon wafers was studied. For a series of mixed brushes with a fixed PMMA M_n and systematically changed PS M_n, a transition in water advancing contact angle (θ_a) from 74°, the value for a flat PMMA surface, to 91°, the value for a flat PS film, was observed with increasing PS M_n after treatment with $CHCl_3$. Atomic force microscopy studies showed smooth surfaces for all samples. While no significant changes in surface morphologies were observed after treatment with cyclohexane, a selective solvent for PS, contact angle and XPS studies indicated that the mixed brushes with a PS M_n slightly smaller than that of PMMA underwent self-reorganization, exhibiting a different θ_a. Intriguing surface morphologies composed of relatively ordered nanoscale domains were found from mixed brushes with PS M_n slightly smaller than or similar to that of PMMA after treatment with acetic acid, a selective solvent for PMMA. The nanodomains are speculated to be of a micellar structure, with PS chains forming a core shielded by PMMA chains.

Introduction

The fabrication of nanometer-scale structures has become an extremely active research area as it is the basis of the emerging nanotechnologies.[1−15] Generally, there are two broadly defined strategies to fabricate nanoscale structures: the so-called top-down and bottom-up methods.[1,2] The top-down approaches, e.g., photolithography,[4] typically begin with a suitable material, and physical means are used to generate patterns from it. The bottom-up methods usually first form the building blocks, e.g., molecules, nanoparticles, etc., and assemble them into the desired structures. With the photolithographic methods reaching the theoretical limits, it becomes increasingly difficult to extend the techniques to the fabrication of patterns with feature sizes below 100 nm, though progress has been made in the development of other lithographic techniques such as electron beam and imprint lithographies.[5,6] Bottom-up approaches are thus receiving growing attention.[1,2] One bottom-up method that has been practiced for many years is self-assembly,[1,2,7−10] which can be defined as well-defined structures resulting spontaneously from the components of a system by noncovalent forces.[2]

Many polymers are "natural" materials for the bottom-up fabrication of nanoscale structures as the dimensions of ordered morphologies fall into the range of 10−200 nm.[9] For instance, block copolymers exhibit a variety of ordered phases including spherical, cylindrical, lamellar, and gyroid morphologies in bulk state.[2,11] Self-assembled diblock copolymers have been used as templates to fabricate dense periodic arrays of nanoscale holes and dots in a silicon wafer,[12] ultrahigh-density nanowire arrays,[13] ordered bicontinuous nanoporous and nanorelief ceramic films,[14] and patterned metal nanoparticles.[15] One type of polymeric materials that has been theoretically predicted to be promising in the bottom-up fabrication of nanoscale structures but has not been extensively experimentally investigated is surface-tethered polymer brushes, which are defined as an assembly of macromolecular chains densely tethered by one end to a surface.[16−19]

† University of Tennessee at Knoxville.
‡ University of Illinois.

(1) Service, R. F. *Science* **2001**, *293*, 782−785.
(2) Forster, S.; Plantenberg, T. *Angew. Chem., Int. Ed.* **2002**, *41*, 688−714.
(3) von Werne, T. A.; Germack, D. S.; Hagberg, E. C.; Sheares, V. V.; Hawker, C. J.; Carter, K. R. *J. Am. Chem. Soc.* **2003**, *125*, 3831−3838.
(4) Wallraff, G. M.; Hinsberg, W. D. *Chem. Rev.* **1999**, *99*, 1801−1821.
(5) Chou, S. Y.; Krauss, P. R.; Renstrom, P. J. *J. Vac. Sci. Technol., B* **1996**, *14*, 4129−4133.
(6) Chou, S. Y.; Krauss, P. R.; Renstrom, P. J. *Science* **1997**, *276*, 1401−1404.
(7) Whitesides, G. M.; Grzybowski, B. *Science* **2002**, *295*, 2418−2421.
(8) Ikkala, O.; ten Brinke, G. *Science* **2002**, *295*, 2407−2409.
(9) Hamley, I. W. *Nanotechnology* **2003**, *14*, R39−R54.
(10) Glass, R.; Moller, M.; Spatz, J. P. *Nanotechnology* **2003**, *14*, 1153−1160.
(11) Bates, F. S.; Fredrickson, G. H. *Annu. Rev. Phys. Chem.* **1990**, *41*, 525−557.
(12) Park, M.; Harrison, C.; Chaikin, P. M.; Register, R. A.; Adadmson, D. H. *Science* **1997**, *277*, 1232−1237.
(13) Thurn-Albrecht, T.; Schotter, J.; Kastle, C. A.; Emley, N.; Shibauchi, T.; Krusin- Elbaum, L.; Guarini, K.; Black, C. T.; Tuominen, M. T.; Russell, T. P. *Science* **2000**, *290*, 2126−2129.
(14) Chan, V. Z. H.; Hoffman, J.; Lee, V. Y.; Iatrou, H.; Avgeropoulos, A.; Hadjichristidis, N.; Miller, R. D.; Thomas, E. L. *Science* **1999**, *286*, 1716−1719.
(15) Lopes, W. A.; Jaeger, H. M. *Nature* **2001**, *414*, 735−738.
(16) Halperin, A.; Tirrell, M.; Lodge, T. P. *Adv. Polym. Sci.* **1992**, *100*, 31−71.
(17) Milner, S. T. *Science* **1991**, *251*, 905−914.
(18) Zhao, B.; Brittain, W. J. *Prog. Polym. Sci.* **2000**, *25*, 677−710.
(19) Russell, T. P. *Science* **2002**, *297*, 964−967.

10.1021/ja049570f CCC: $27.50

Theoretical studies have been performed on a wide range of polymer brush systems,[20,21] and many interesting nanoscale structures have been suggested.

Of special interest here are binary mixed homopolymer brushes composed of two distinct homopolymers randomly or alternatively immobilized on a surface with high grafting densities.[21−28] Theoretical studies have discussed whether symmetric mixed homopolymer brushes on a planar substrate phase separate laterally forming a "rippled" state or vertically resulting in a "layered" state under equilibrium melt conditions, and the studies have suggested that the "rippled" state should be the one to appear.[21] The spatial period of the pattern is predicted to be on the order of the polymer chain root-mean-square end-to-end distance, though it is unknown what kinds of patterns will form. The self-assembly of mixed brushes upon exposure to solvents is also of great interest.[22−27] Layered structures may form in asymmetric binary polymer brushes.[24] Micellar structures with the solvophobic chains associating into a dense core and the solvophilic chains forming an outer shell have been predicted to form in selective solvents.[25,26] Since the solvophilic chains extend into the solution and their density decays from the core of the solvophobic chains, these surface micelles have a "flowerlike" appearance.[25] By tuning parameters including molecular weights, chain compositions, grafting densities, solvents, and temperature, various nanoscale patterns could be achieved by mixed homopolymer brushes. Experimental studies on mixed polymer brushes began very recently, and both "grafting to" and "grafting from" methods have been used to fabricate various mixed brushes on flat substrates.[28−31] It is worth noting that "grafting from" initiator-terminated self-assembled monolayers (SAMs) by use of controlled/"living" polymerization techniques has emerged as a powerful method to synthesize dense polymer brushes with controlled molecular weights and relatively narrow polydispersities.[18,30−32] In previous publications, we reported the synthesis of mixed poly(methyl methacrylate) (PMMA)/polystyrene (PS) brushes on planar silica substrates from either mixed initiator-terminated SAMs[30] or an asymmetric difunctional initiator-terminated SAM (Y-SAM) by combining atom transfer radical polymerization (ATRP) and nitroxide-mediated radical polymerization (NMRP).[31] Inspired by the theoretical predictions, we are exploring the formation of nanoscale patterns from mixed brushes by considering the effects of molecular weight, grafting density, solvent, and temperature. In this article, we report our studies on the molecular weight dependence of solvent-induced self-assembly of mixed PMMA/PS brushes on silicon wafers. Contact angle measurements, atomic force microscopy (AFM), and X-ray photoelectron spectroscopy (XPS) were used to characterize the mixed brushes after treatment with different solvents.

Results and Discussion

Synthesis of Mixed PMMA/PS Brushes on Planar Silica Substrates. Mixed PMMA/PS brushes with various molecular weights used in present studies were synthesized from a Y-SAM by combining ATRP and NMRP in a two-step process (Scheme 1). The details of the procedure were described in the Supporting Information of a previous publication.[31] Y-SAM was designed to ensure that the two initiators were well-mixed in the monolayer at a molecular level. ATRP and NMRP are two different controlled radical polymerization techniques and are performed at different polymerization conditions.[33,34] We chose ATRP to synthesize the first polymer and NMRP for the second polymer because the activation of an ATRP initiator with a metal complex is a bimolecular process, while the free radicals in NMRP are formed by thermal decomposition, which is a unimolecular process. A unimolecular activation mechanism is preferred for the synthesis of the second type of polymer chains from the surface because of the steric hindrance presented by the existing polymer chains. Surface-initiated ATRP of MMA was carried out at 75 °C using CuBr and *N*,*N*′,*N*′,*N*″-pentamethyldiethylenetriamine as catalytic system. We confirmed that the NMRP initiator was stable under the ATRP conditions. A "free" ATRP initiator, ethyl 2-bromoisobutyrate,was added into the reaction systems to control the polymerizations.[32c]

(20) (a) Alexander, S. *J. Phys. (Paris)* **1977**, *38*, 977−981. (b) de Gennes, P. G. *Macromolecules* **1980**, *13*, 1069−1075. (c) Pincus, P. *Macromolecules* **1991**, *24*, 2912−2919. (d) Zhulina, E. B.; Singh, C.; Balazs, A. C. *Macromolecules* **1996**, *29*, 6338−6348. (e) Zhulina, E. B.; Singh, C.; Balazs, A. C. *Macromolecules* **1996**, *29*, 8254−8259. (f) Amoskov, V. M.; Birshtein, T. M.; Pryamitsyn, V. A. *Macromolecules* **1996**, *29*, 7240−7250.

(21) (a) Marko, J. F.; Witten, T. A. *Phys. Rev. Lett.* **1991**, *66*, 1541−1544. (b) Dong, H. *J. Phys. II* **1993**, *3*, 999−1020. (c) Marko, J. F.; Witten, T. A. *Macromolecules* **1992**, *25*, 296−307. (d) Brown, G.; Chakrabarti, A.; Marko, J. F. *Europhys. Lett.* **1994**, *25*, 239−244.

(22) Zhulina, E.; Balazs, A. C. *Macromolecules* **1996**, *29*, 2667−2673.

(23) Soga, K. G.; Zuckermann, M. J.; Guo, H. *Macromolecules* **1996**, *29*, 1998−2005.

(24) Lai, P.-Y. *J. Chem. Phys.* **1994**, *100*, 3351−3357.

(25) Singh, C.; Pickett, G. T.; Balazs, A. C. *Macromolecules* **1996**, *29*, 7559−7570.

(26) Singh, C.; Zhulina, E. B.; Gersappe, D.; Pickett, G. T.; Balazs, A. C. *Macromolecules* **1996**, *29*, 7637−7640.

(27) Muller, M. *Phys. Rev. E* **2002**, *65*, 030802.

(28) Minko, S.; Muller, M.; Usov, D.; Scholl, D.; Froeck, C.; Stamm, M. *Phys. Rev. Lett.* **2002**, *88*, 035502.

(29) (a) Sidorenko, A.; Minko, S.; Schenk-Meuser, K.; Duschner, H.; Stamm, M. *Langmuir* **1999**, *24*, 8349−8355. (b) Minko, S.; Usov, D.; Goreshnik, E.; Stamm, M. *Macromol. Rapid. Commun.* **2001**, *22*, 206−211. (c) Minko, S.; Muller, M.; Motornov, M.; Nitschke, M.; Grundke, K.; Stamm, M. *J. Am. Chem. Soc.* **2003**, *125*, 3896−3900. (d) Minko, S.; Luzinov, I.; Luchnikov, V.; Muller, M.; Patil, S.; Stamm, M. *Macromolecules* **2003**, *36*, 7268−7279. (e) Julthongpiput, D.; Lin, Y. H.; Teng, J.; Zubarev, E. R.; Tsukruk, V. V. *Langmuir* **2003**, *19*, 7832−7836. (f) Lemieux, M.; Usov, D.; Minko, S.; Stamm, M.; Shulha, H.; Tsukruk, V. V. *Macromolecules* **2003**, 36, 7244−7255. (g) Ionov, L.; Minko, S.; Stamm, M.; Gohy, J. F.; Jerome, R.; Scholl, A. *J. Am. Chem. Soc.* **2003**, *125*, 8302−8306. (h) Houbenov, N.; Minko, S.; Stamm, M. *Macromolecules* **2003**, *36*, 5897−5901.

(30) Zhao, B. *Polymer* **2003**, *44*, 4079−4083.

(31) Zhao, B.; He, T. *Macromolecules* **2003**, *36*, 8599−8602.

(32) (a) Huang, X. Y.; Wirth, M. J. *Anal. Chem.* **1997**, *69*, 4577−4580. (b) Jordan, R.; Ulman, A. *J. Am. Chem. Soc.* **1998**, *120*, 243−247. (c) Husseman, M.; Malmstrom, E. E.; McNamara, M.; Mate, M.; Mecerreyes, D.; Benoit, D. G.; Hedrick, J. L.; Mansky, P.; Huang, E.; Russell, T. P.; Hawker, C. J. *Macromolecules* **1999**, *32*, 1424−1431. (d) Zhao, B.; Brittain, W. J. *J. Am. Chem. Soc.* **1999**, *121*, 3557−3558. (e) Matyjaszewski, K.; Miller, P. J.; Shukla, N.; Immaraporn, B.; Gelman, A.; Luokala, B. B.; Siclovan, T. M.; Kickelbick, G.; Vallant, T.; Hoffmann, H.; Pakula, T. *Macromolecules* **1999**, *32*, 8716−8724. (f) Pyun, J.; Kowalewski, T.; Matyjaszewski, K. *Macromol. Rapid. Commun.* **2003**, *24*, 1043−1059. (g) Ejaz, M.; Yamamoto, S.; Ohno, K.; Tsujii, Y.; Fukuda, T. *Macromolecules* **1998**, *31*, 5934−5936. (h) Kim, J.-B.; Bruening, M. L.; Baker, G. L. *J. Am. Chem. Soc.* **2000**, *122*, 7616−7617. (i) von Werne, T.; Patten, T. E. *J. Am. Chem. Soc.* **2001**, *123*, 7497−7505. (j) Boyes, S. G.; Brittain, W. J.; Weng, X.; Cheng, S. Z. D. *Macromolecules* **2002**, *35*, 4960−4967. (k) Wu, T.; Efimenko, K.; Genzer, J. *J. Am. Chem. Soc.* **2002**, *124*, 9394−9395. (l) Advincular, R.; Zhou, Q. G.; Park, M.; Wang, S. G.; Mays, J.; Sakellariou, G.; Pispas, S.; Hadjichristidis, N. *Langmuir* **2002**, *18*, 8672−8684. (m) Quirk, R. P.; Mathers, R. T.; Cregger, T.; Foster, M. D. *Macromolecules* **2002**, *35*, 9964−9974. (n) Husemann, M.; Mecerreyes, D.; Hawker, C. J.; Hedrick, J. L.; Shah, R.; Abbott, N. L. *Angew. Chem., Int. Ed.* **1999**, *38*, 647−649. (o) Lahann, J.; Langer, R. *Macromol. Rapid Commun.* **2001**, *22*, 968−971. (p) Kim, N. Y.; Jeon, N. L.; Choi, I. S.; Takami, S.; Harada, Y.; Finnie, K. R.; Girolami, G. S.; Nuzzo, R. G.; Whitesides, G. M.; Laibinis, P. E. *Macromolecules* **2000**, *33*, 2793−2795. (q) Jones, D. B.; Brown, A. A.; Huck, W. T. S. *Langmuir* **2002**, *18*, 1265−1269. (r) Schmidt, R.; Zhao, T. F.; Green, J. B.; Dyer, D. J. *Langmuir* **2002**, *18*, 1281−1287.

(33) (a) Matyjaszewski, K.; Xia, J. H. *Chem. Rev.* **2001**, *101*, 2921−2990. (b) Hawker, C. J.; Bosman, A. W.; Harth, E. *Chem. Rev.* **2001**, *101*, 3661−3688.

(34) He, T.; Li, D. J.; Sheng, X.; Zhao, B. *Macromolecules* **2004**, in press.

Scheme 1. Synthesis of Mixed PMMA/PS Brushes from an Asymmetric Difunctional Initiator-Terminated SAM (Y-SAM) by Combining ATRP and NMRP Techniques

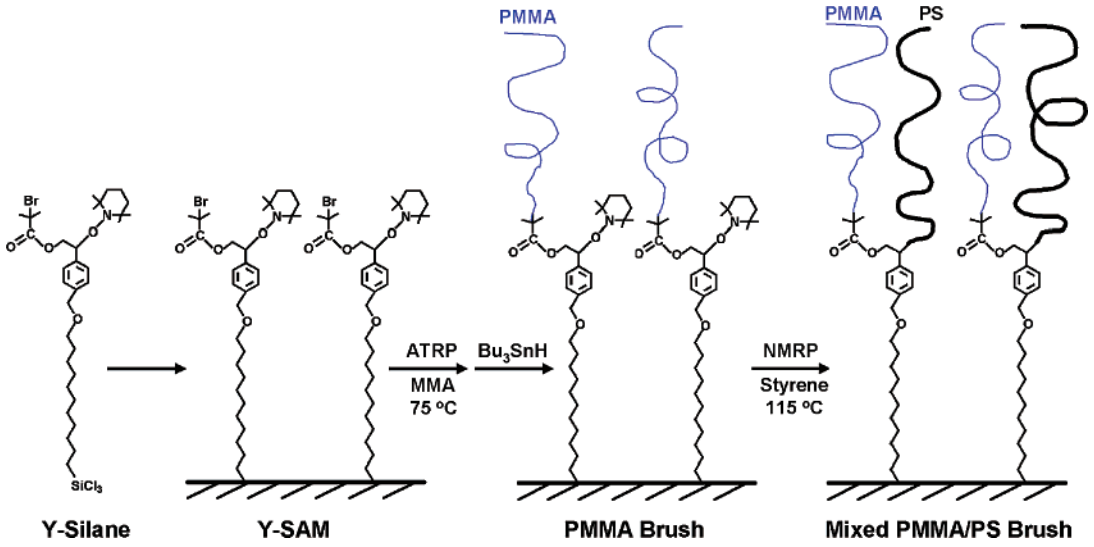

The polymers formed in the solutions were collected and analyzed by gel permeation chromatography (GPC) using PS standards. We assume that the molecular weights and the polydispersities of the grafted polymers are identical to those of "free" polymers. The studies by other researchers by cleaving the polymer chains off high surface area silica gels indicated that the molecular weights and polydispersities of the grafted polymers and "free" polymers were close.[32c] It was observed that the thickness of the brushes increased linearly with the molecular weight of "free" PMMA, suggesting that the polymerizations were well-controlled.

The silicon wafers were then cut into smaller pieces and subjected to NMRP conditions (bulk styrene at 115 °C in the presence of a "free" initiator, 1-phenyl-1-(2′,2′,6′,6′-tetramethyl-1′-piperidinyloxy)-2-benzoyloxyethane) for various amounts of time. "Free" polystyrenes produced in the solutions were collected and analyzed by GPC. The film thickness increased with the PS M_n in an almost linear fashion. To confirm that PS chains were initiated from the NMRP initiator, we exposed a 17.8 nm PMMA brush that was synthesized from the SAM of 11′-trichlorosilylundecyl 2-bromo-2-methylpropionate (ATRP-silane, an ATRP initiator) to the typical NMRP conditions. No noticeable changes were observed in the thickness and water contact angles. However, when exposing a SAM of ATRP-silane and a mixed SAM that was prepared from a toluene solution containing ATRP-silane and 1-(3′-oxa-2′-phenyl-14′-trichlorosilyltetradecyloxy)-2,2,6,6-tetramethyl-piperidine (NMRP-silane, a NMRP initiator) with a molar ratio of 54.4:45.6 to the NMRP conditions, we observed a ~2.0 nm film thickness increase and a water advancing contact angle of 91°, the value for flat PS films,[35] on the SAM of ATRP-silane, while a 19.1 nm brush was found from the mixed SAM. Presumably, the C−Br bond in the ATRP initiator was weak and acted as a chain transfer agent in NMRP. To eliminate the possible chain transfers to bromine-terminated PMMA chain ends and the unreacted ATRP initiator in Y-SAM in the synthesis of PS by NMRP, tri-*n*-butyltin hydride (*n*-Bu_3SnH) was added into the reaction mixtures to remove bromine atoms in situ after ATRP.[36] Control experiments demonstrated that exposing a SAM of ATRP-silane and a 10.2 nm PMMA brush grown from Y-SAM to the typical dehalogenation conditions for 10 and 30 min, respectively, completely removed bromine atoms as subsequently attempted ATRPs resulted in no changes in the film thicknesses and water contact angles. We also confirmed that the NMRP initiator in Y-SAM was stable under the typical dehalogenation conditions. Considering that these mixed brushes were composed of PMMA and PS with various molecular weights, it was difficult to determine the thicknesses by ellipsometry as it was unclear at this stage at what molecular weights PMMA and PS chains in the mixed brushes would phase-separate and what kind of structures would form if phase separation occured. To estimate the film thickness, we used a refractive index of 1.49 for all mixed PMMA/PS brushes (the refractive index of PS is 1.59).

Samples with various molecular weights for PMMA and PS chains were used in the present studies of self-assembly in different solvents: chloroform, cyclohexane, and glacial acetic acid. Chloroform is a good solvent for both PMMA and PS. Cyclohexane is a good solvent for PS at temperatures above 35 °C but a poor solvent for PMMA chains. Glacial acetic acid is a selective solvent for PMMA.[37]

Self-Assembly of Mixed PMMA/PS Brushes Induced by Cyclohexane. A set of mixed brushes composed of PMMA with a fixed M_n of 17 500 ($M_w/M_n = 1.15$) and PS with M_n ranging from 4300 to 26 100 was used in the study of self-assembly induced by cyclohexane. The molecular weight of PS and the thickness for each sample are summarized in Table 1. The samples were first treated with chloroform at room temperature for 5 min and dried with a stream of clean air, followed by characterization with contact angle measurements, AFM, and

(35) Slightly different contact angle values may be obtained for the same surface if different methods, e.g., Wilhelmy balance, tilting plate, or the sessile drop techniques, are used in contact angle measurements. See: Lander, L. M.; Siewierski, L. M.; Brittain, W. J.; Vogler, E. A. *Langmuir* **1993**, *9*, 2237−2239. In the present study, we used the sessile drop method (see Supporting Information). Advancing and receding contact angles were recorded while water was added to and withdrawn from the water drop via a syringe, respectively.

(36) Coessens, V.; Matyjaszewski, K. *Macromol. Rapid Commun.* **1999**, *20*, 66−70.

(37) Brandrup, J.; Immergut, E. H. *Polymer Handbook*, 3rd ed.; John Wiley & Sons: New York, 1989.

Table 1. Mixed PMMA/PS Brushes after Sequential Treatments with Chloroform, Cyclohexane, and Chloroform[a]

no.	PS M_n	PS M_w	d[b] (nm)	θ_a, θ_r (deg) after $CHCl_3$[c]	θ_a, θ_r (deg) after Cyc[d]	θ_a, θ_r (deg) after $CHCl_3$[e]	O % Cyc[f]	O % $CHCl_3$[g]
1	4300	5600	17.6	74, 62	74, 62	74, 65	22.06	29.69
2	11 100	14 500	24.9	77, 69	92, 81	78, 68	8.74	17.74
3	13 100	16 700	27.0	79, 70	92, 83	80, 69	9.00	15.37
4	14 000	17 500	28.3	83, 71	91, 83	82, 73	6.84	11.25
5	20 100	25 600	33.5	91, 83	91, 84	91, 83	1.27	3.26
6	26 100	33 600	42.8	91, 83	91, 84	91, 83	0.88	3.23

[a] The M_n and M_w of PMMA were 17 500 and 20 200, respectively. The thickness of PMMA brush (before NMRP) was 14.8 nm. [b] d = thickness (nm). [c] The samples were treated with $CHCl_3$ at room temperature for 5 min and dried immediately with an air stream, followed by water contact angle measurements. θ_a and θ_r are water advancing and receding contact angles, respectively. [d] Cyc = cyclohexane. The samples were then treated with cyclohexane at 45 °C for 30 min and dried immediately with an air stream, followed by water contact angle measurements. No changes in water contact angles were observed after treatment again with cyclohexane at 45 °C for 30 min. [e] The samples were treated with chloroform again at room temperature for 5 min and dried with an air stream, followed by water contact angle measurements. [f,g] The oxygen atomic compositions obtained from XPS measurements after treatment with cyclohexane and chloroform, respectively. C % + O % = 100%.

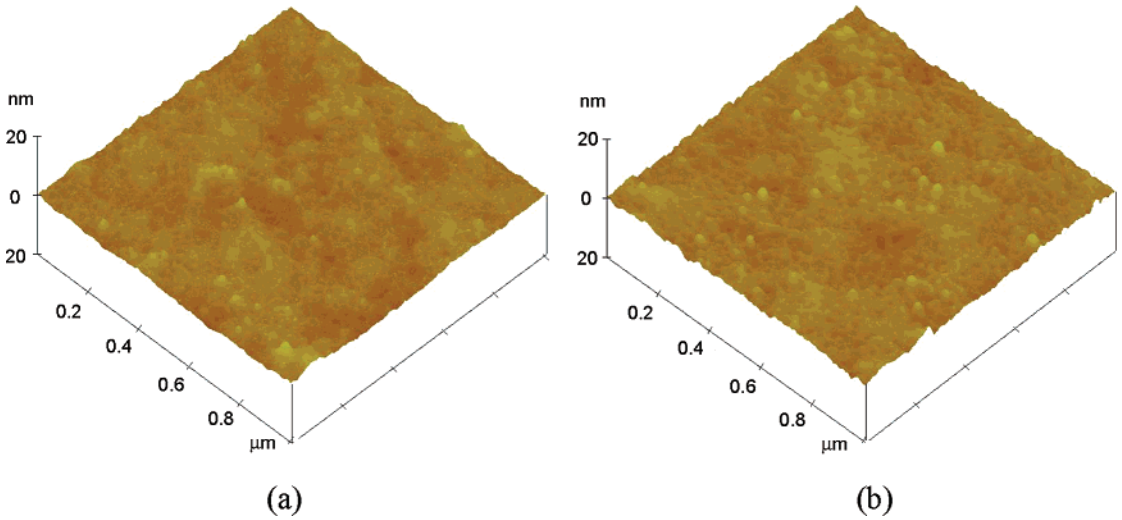

Figure 1. AFM images of sample **3** after treatment with $CHCl_3$ at room temperature for 5 min (a), and after treatment with cyclohexane at 45 °C for 60 min (b) followed by drying with a stream of air.

Scheme 2. Schematic Illustration of Mixed Brushes Composed of PMMA with a Fixed M_n and PS with Various Molecular Weights after Treatment with Chloroform

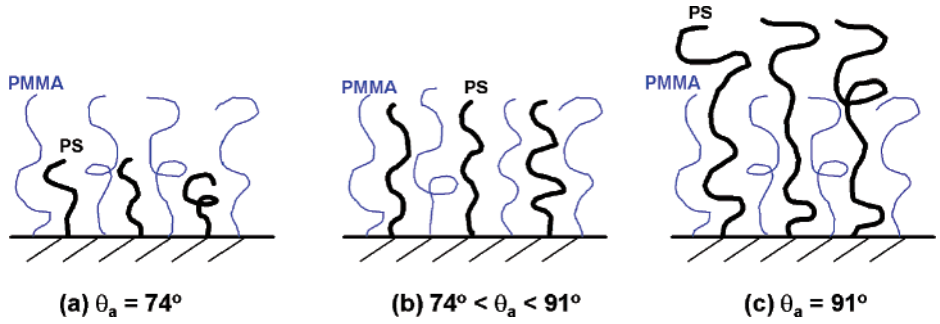

XPS. AFM imaging showed a smooth surface morphology for all six samples with a root-mean-square surface roughness on the order of 0.5 nm (Figure 1a shows the AFM image of sample **3**).

It was observed that the advancing contact angle (θ_a) of water on these mixed brushes after treatment with chloroform exhibited a transition from 74°, the value of water θ_a on a flat PMMA surface, to 91°, the value for flat PS films, with the increase of the molecular weight of PS. When the PS chain was much shorter than that of PMMA, e.g., in sample **1**, the surface exhibited the same values of water contact angles as a pure flat PMMA film as the outermost layer was occupied by PMMA chains (Scheme 2). When the M_n of PS was slightly smaller than that of PMMA, the water θ_a was found to be between 74° and 91° (samples **2**−**4**). Since the surface was flat as shown in Figure 1a, a value between 74° and 91° for water θ_a can be interpreted that both polymers were present in the sensing region of the probing liquid water. When the M_n of PS was higher than that of PMMA, the water θ_a was 91°, implying that the outermost layer was occupied by PS chains. These observations were also supported by XPS data that were summarized in Table 1. The oxygen content decreased from 29.69% to 3.23% with the molecular weight of PS increasing from 4300 to 26 100. For a pure PMMA brush with a thickness higher than 10 nm, the calculated oxygen content is 28.6%. The XPS spectrum of sample **3** is shown in Figure 2a. It should be

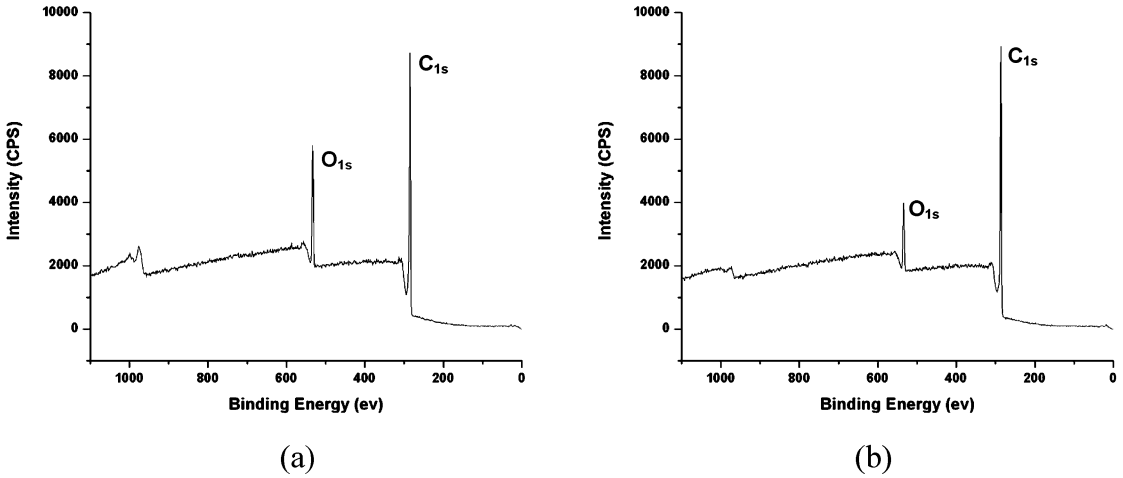

Figure 2. XPS spectra of sample **3** after treatment with $CHCl_3$ (a) and cyclohexane (b).

noted that the takeoff angle in the XPS measurements was 90°. The sampling depths were 7.3 nm for O_{1s} and 8.7 nm for C_{1s} (95% signals), though signals might also come from deeper regions.[38]

The samples were then treated with cyclohexane at 45 °C for 30 min.[39] The water θ_a remained essentially the same for samples **1**, **5**, and **6**, but increased to 92° or 91° for samples **2**−**4**. No changes in water contact angles were observed after treatment again with cyclohexane for 30 min. Unlike the block copolymer brushes,[40] AFM studies showed no significant changes in surface morphologies after treatment with cyclohexane for all samples (Figure 1b shows the AFM image of sample **3**), though there was a small increase in surface roughness (the surface roughness in Figure 1b was 0.65 nm in contrast to 0.57 nm in Figure 1a). Thus, a water θ_a of 91° suggested that the mixed brushes underwent self-reorganization and the outermost layer was dominated by PS chains, which was confirmed by XPS data. The XPS spectrum of sample **3** after treatment with cyclohexane is shown in Figure 2b. The oxygen peak decreased significantly, and a quantitative analysis showed that the oxygen atomic composition of this mixed brush decreased from 15.37% to 9.00%. As mentioned before, cyclohexane is a good solvent for PS at temperatures above 35 °C but a poor solvent for PMMA. The PS chains were swollen by cycohexane, assumed more extended conformations, and moved to the outermost layer. Simultaneously, the PMMA chains moved to the deeper region of the brush to avoid contact with the solvent to minimize the free energy of the whole system (Scheme 3). It can be envisioned that a water θ_a of 91° is observed only when the PS chain is long enough. In our experiments, we found that to achieve a water θ_a of 91°, the PS molecular weight was at least about half of that of PMMA. It is unknown at this stage how the PMMA chains aggregate inside the brushes. The changes of water contact angles observed after treatment with cyclohexane were reversible. After treatment with chloroform again, the samples exhibited essentially the same values of water contact angles as before (Table 1).

Scheme 3. Mixed PMMA/PS Brushes Undergo Reorganization in Response to the Treatment with Cyclohexane, Exhibiting a Different Surface Wettability

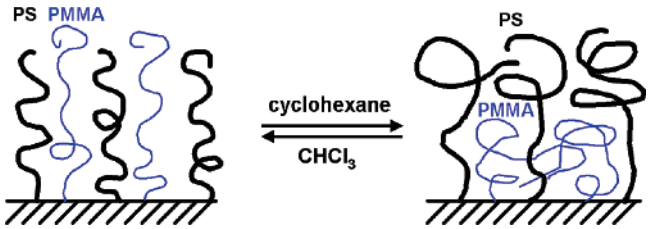

It should be noted that the samples can be damaged by energetic photons and electrons during the XPS measurements as PMMA undergoes degradation upon exposure to X-rays.[38] To minimize the damages, we collected only two sweeps for each survey spectrum. No noticeable changes on the samples were observed. However, after the samples were washed with chloroform, the damages on the thick samples were visible to the naked eye. We speculate that the oligomers produced from the degradation remain in the same positions and the glassy states of the two polymers prevent the removal of the degraded polymer chains. Thus, we believe that the XPS data reflect the compositions of the outermost surfaces of the mixed brushes. The second XPS measurements were taken at a different spot for all samples.

Self-Assembly of Mixed PMMA/PS Brushes Induced by Glacial Acetic Acid. In contrast to cyclohexane, glacial acetic acid (AA) is a selective solvent for PMMA. To study the self-assembly induced by AA, we prepared a new series of samples with various molecular weights for PMMA and PS (Table 2) as the samples in the previous experiments were damaged in XPS measurements. For samples **7**−**11**, the M_n of PMMA was 26 700 (M_w/M_n = 1.19) and the M_n of PS was systematically changed from 3300 to 27 000. To further increase the molecular weight of PS relative to that of PMMA, we included two more samples (samples **12** and **13**). The M_n of PMMA was 19 500 (M_w/M_n = 1.16), and the molecular weights of PS for **12** and **13** were 22 400 and 34 800, respectively. The samples were first treated with chloroform followed by characterization with contact angle measurements, AFM, and XPS. As with the samples in Table 1 after treatment with chloroform, AFM studies showed a smooth surface for all brushes with a surface roughness on the order of 0.5 nm. A transition in water θ_a from

(38) Briggs, D. *Surface Analysis of Polymers by XPS and Static SIMS*; Cambridge University Press: Cambridge, U.K., 1998.
(39) Experimental details are included in the Supporting Information.
(40) (a) Zhao, B.; Brittain, W. J.; Zhou, W. S.; Cheng, S. Z. D. *J. Am. Chem. Soc.* **2000**, *122*, 2407−2408. (b) Zhao, B.; Brittain, W. J.; Zhou, W. S.; Cheng, S. Z. D. *Macromolecules* **2000**, *33*, 8821−8827. (c) Huang, W.; Kim, J.-B.; Baker, G. L.; Bruening, M. L. *Nanotechnology* **2003**, *14*, 1075−1080.

Table 2. Mixed PMMA/PS Brushes with Various Molecular Weights after Sequential Treatments with Chloroform, Glacial Acetic Acid, and Chloroform

no.	PS M_n	PS M_w	d (nm)	θ_a, θ_r (deg) after $CHCl_3$[a]	θ_a, θ_r AA[b] (deg)	θ_a, θ_r AA[c] (deg)	θ_a, θ_r AA[d] (deg)	θ_a, θ_r (deg) $CHCl_3$[e]
7[f]	3300	4300	23.1	74, 63	76, 50	88, 65	88, 60	74, 64
8[f]	17 900	22 100	41.2	79, 71	92, 32	91, 31	91, 30	79, 71
9[f]	19 000	23 600	43.3	82, 71	92, 30	92, 30	92, 31	81, 71
10[f]	23 700	29 700	48.0	86, 76	96, 32	96, 33	96, 32	86, 76
11[f]	27 000	33 400	54.2	91, 83	96, 49	100, 42	100, 42	91, 83
12[g]	22 400	29 600	42.0	91, 84	92, 64	94, 59	95, 63	91, 84
13[g]	34 800	44 800	54.8	91, 85	95, 72	97, 73	97, 73	91, 83
14	PMMA brush		18.1	74, 65	81, 57	83, 55	84, 55	74, 64

[a] The samples were immersed in chloroform for 5 min and dried immediately with a stream of air, followed by water contact angle measurements. θ_a and θ_r are water advancing and receding contact angles, respectively. [b] The samples were treated with glacial acetic acid (AA) at 45 °C for 30 min, washed with water, and dried with an air stream, followed by water contact angle measurements. [c,d] The samples were treated with AA for the second and third times at 45 °C for 30 min. [e] The samples were treated in chloroform again for 5 min and dried immediately with a stream of air, followed by water contact angle measurements. [f] The M_n and M_w of PMMA (samples **7**−**11**) were 26 700 and 31 700, respectively; the thickness of PMMA brush (before NMRP) was 21.0 nm. [g] The M_n and M_w of PMMA were 19 500 and 22 700, respectively. The thickness of PMMA brush (before NMRP) was 14.5 nm.

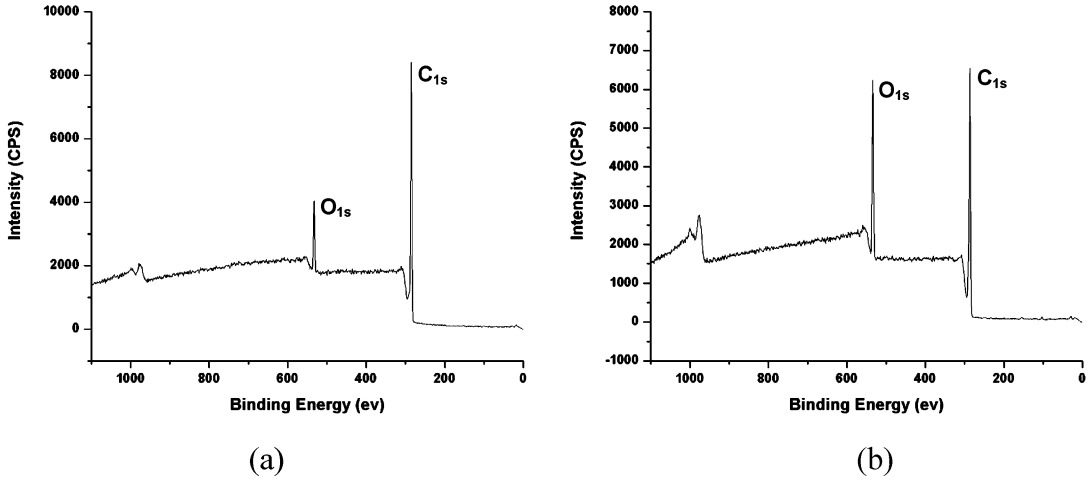

Figure 3. XPS spectra of sample **9** after treatment with $CHCl_3$ (a) and glacial acetic acid (b).

Table 3. Oxygen Atomic Compositions of Samples **7**−**13** after Treatments with $CHCl_3$ and Glacial Acetic Acid (AA)

sample no.	**7**	**8**	**9**	**10**	**11**	**12**	**13**
after $CHCl_3$ (O %)[a]	28.42	10.94	7.64	8.17	5.69	4.47	3.64
after AA (O %)[a]	25.92	19.20	18.54	16.25	13.42	12.13	8.16

[a] O % + C % = 100%.

74° to 91° was observed with increasing the molecular weight of PS, which was also supported by XPS data (Table 3). The oxygen atomic composition decreased from 28.42% (sample **7**) to 3.64% (sample **13**).

The samples were then immersed in AA at 45 °C for 30 min and washed with water to remove acetic acid, followed by drying with a stream of air.[39] This process was repeated twice, and no noticeable changes in water contact angles were observed after treatment for the third time. Unlike in the treatment with cyclohexane, where 91°, the value of water θ_a on a flat PS surface, was observed for mixed brushes with PS M_n slightly less than that of PMMA, we did not observe 74°, the value of water θ_a on a flat PMMA surface, on any brush in Table 2. Even for sample **7** in which the M_n of PMMA (26 700) was much higher than that of PS (3300), the advancing and receding contact angles of water were 88° and 60°, respectively, after treatment with AA three times. With the increase of the molecular weight of PS, the water θ_a gradually increased, and the highest value, 100°, was found when the M_n of PS was 27 000 (sample **11**), which was very close to that of PMMA (M_n = 26 700). The receding contact angles of water on samples **8**−**11** were in the range of 30−42°. The contact angle hystereses for these samples were very high, ∼60°, implying that the surfaces might be very rough, though chemical heterogeneity can also contribute to the hysteresis. With a further increase in the PS molecular weight relative to that of PMMA, the contact angle hysteresis decreased to 32° (sample **12**) and 24° (sample **13**), implying that the surface roughness might become smaller.

XPS studies confirmed that the PMMA chains were enriched at the air−brush interfaces after treatments with AA except for the sample **7** where the lower oxygen content might come from an experimental error (Table 3). The XPS spectra of sample **9** are shown in Figure 3. It was observed that the oxygen peak increased significantly after treatment with AA compared to that after treatment with $CHCl_3$. Quantitative analyses showed that the oxygen contents were 7.64% and 18.54% after $CHCl_3$ and AA, respectively. For samples **7**−**13**, the oxygen content continuously decreased from 25.92% (sample **7**) to 8.16% (sample **13**) with the increase of the molecular weight of PS relative to that of PMMA after treatment by AA (Table 3).

The increase in water θ_a and the decrease in water θ_r on the mixed brush **7** cannot be attributed to the presence of PS chains in the sensing depth of water in contact angle measurements as the PS chain was too short to reach the air−brush interface. In a control experiment, we treated a 18.1 nm pure PMMA brush (sample **14** in Table 2) with AA by the same conditions. It was observed that the water θ_a and θ_r changed to 81° and 57° after treatment once and stabilized at 84° and 55° after treatment two

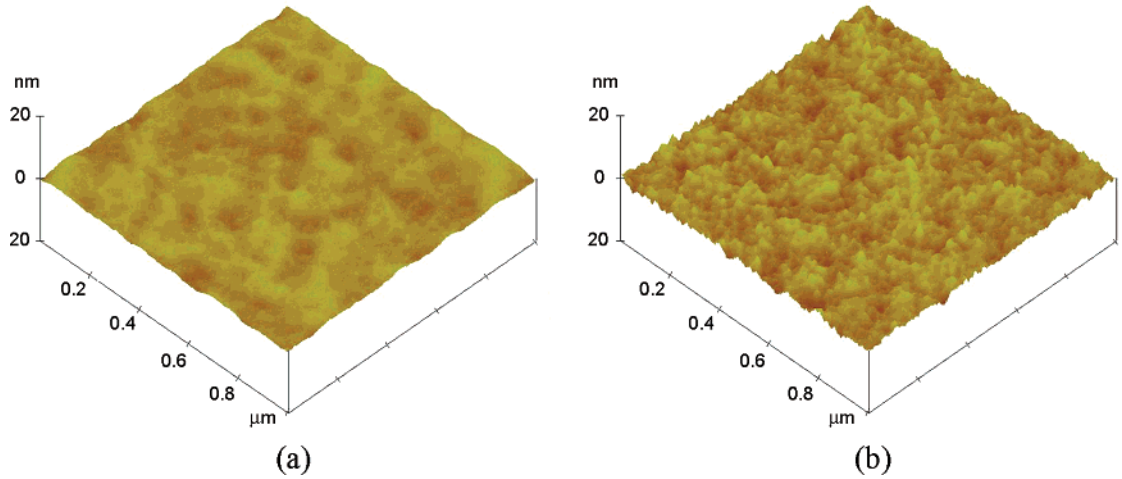

Figure 4. AFM images of a pure PMMA brush (sample **14**) after treatment with $CHCl_3$ (a) and glacial acetic acid (b).

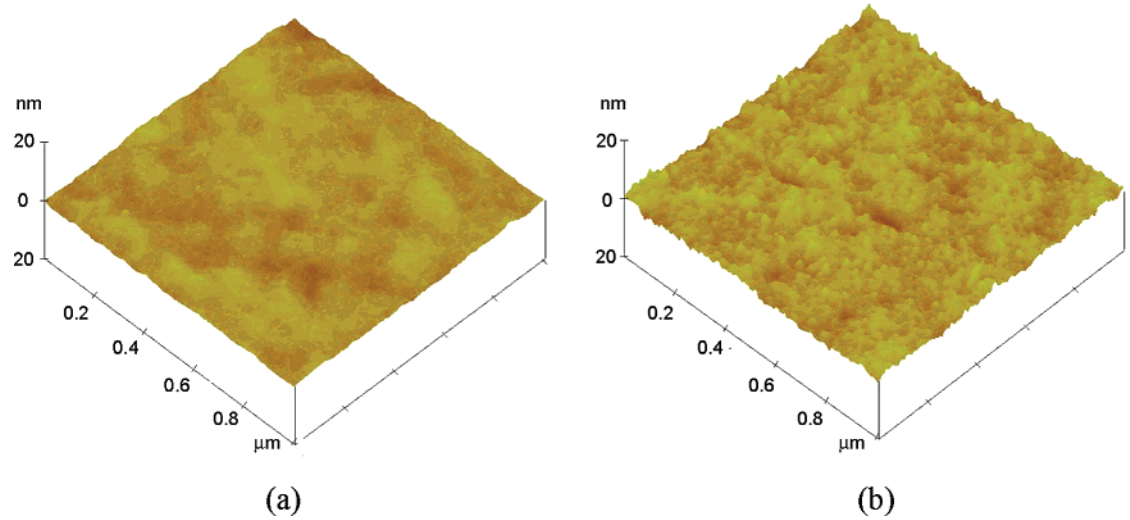

Figure 5. AFM images of sample **7** after treatment with $CHCl_3$ (a) and glacial acetic acid (b).

more times. Higher contact angle hystereses (29° for the pure PMMA brush and 28° for sample **7**) compared to those after treatment with chloroform (~10°) implied that the surfaces might become rough, which was confirmed by AFM studies. Figures 4 and 5 show the images of samples **14** and **7** after treatments with chloroform and AA, respectively. The surface roughness increased from 0.42 nm (Figure 4a) to 0.78 nm (4b), and from 0.51 nm (5a) to 0.82 nm (5b).

The apparent contact angle values can be influenced by both surface chemical composition and surface roughness.[41] The effect of surface roughness on apparent contact angle values is usually described by the Wenzel equation: $\cos\theta^* = r\cos\theta$, where θ is the Young intrinsic contact angle on a flat homogeneous surface, θ^* is the apparent contact angle on a rough surface, and r is the surface roughness defined as the ratio of the actual surface area over the projected surface area.[41] Wenzel's equation states that the surface roughness improves the wettability for a hydrophilic surface but makes it worse for a hydrophobic surface. However, our observations cannot be explained by this equation. It is known that the surface roughness can influence the apparent contact angles through many different and subtle ways.[42,43] Although the ultrahydrophobic surfaces have been successfully designed and fabricated by manipulation of surface roughness and surface chemical composition,[44] less attention has been paid to how surface roughness affects the apparent contact angle in the hydrophilic region when the inherent water contact angle is lower than 90°. Recently, Herminghaus' theoretical studies indicated that it is possible to fabricate a water-repellent surface from a material with an intrinsic contact angle less than 90°.[43] Feng et al. successfully created a superhydrophobic surface from poly(vinyl alcohol) whose intrinsic water contact angle was 72°.[45] More efforts are needed to explain these observations.

Figures 6−11 show the AFM images (3-D and 2-D images, and the cross-sectional profile along the line in the 2-D image) of samples **8**−**13** after treatment with AA three times. For samples **8** to **11**, very rough surfaces composed of nanoscale domains were observed, consistent with the observations in the study of water contact angles. For samples **8** and **9**, the surface

(41) (a) Adamson, A. W.; Gast, A. P. *Physical Chemistry of Surfaces*, 6th ed.; John Wiley & Sons: New York, 1997; p 358. (b) Wenzel, R. N. *Ind. Eng. Chem.* **1936**, *28*, 988−994.

(42) (a) Johnson, R. E., Jr.; Dettre, R. H. *Adv. Chem. Ser.* **1964**, *43*, 112−135. (b) Dettre, R. H.; Johnson, R. E., Jr. *Adv. Chem. Ser.* **1964**, *43*, 136−144.
(43) Herminghaus, S. *Europhys. Lett.* **2000**, *52*, 165−170.
(44) (a) Onda, T.; Shibuichi; Satoh, N.; Tsujii, K. *Langmuir* **1996**, *12*, 2125−2127. (b) Bico, J.; Marzolin, C.; Quéré, D. *Europhys. Lett.* **1999**, *47*, 220−226. (c) Oner, D.; McCarthy, T. J. *Langmuir* **2000**, *16*, 7777−7782.
(45) Feng, L.; Song, Y.; Zhai, J.; Liu, B.; Xu, J.; Jiang, L.; Zhu, D. *Angew. Chem. Int. Ed.* **2003**, *42*, 800−802.

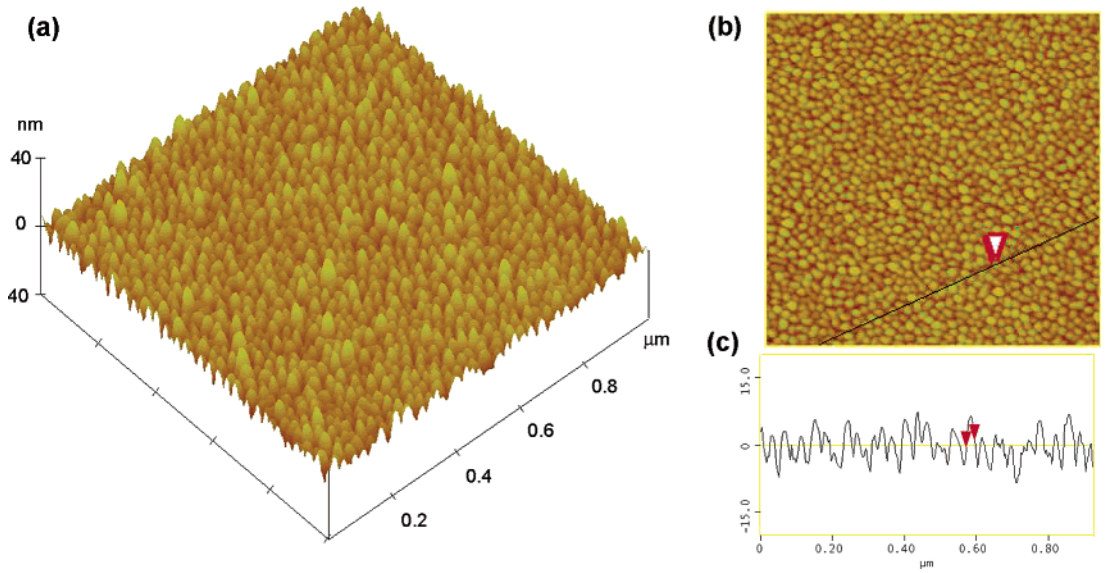

Figure 6. AFM images of sample **8** after treatment with glacial acetic acid. (a) 3-D image. (b) 2-D top-view image. (c) Cross-sectional profile along the line in image (b).

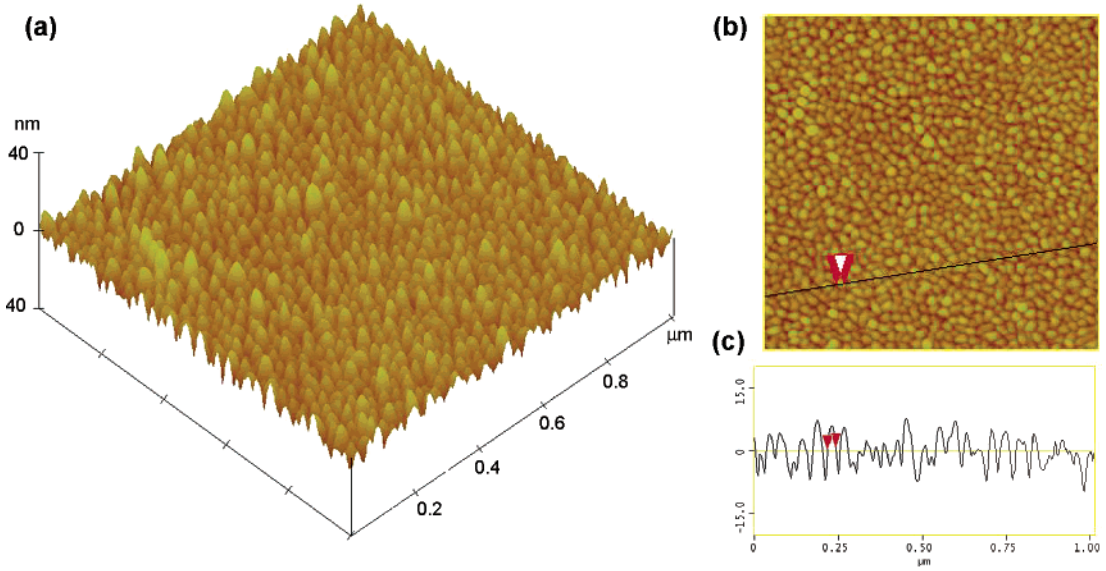

Figure 7. AFM images of sample **9** after treatment with glacial acetic acid. (a) 3-D image. (b) 2-D top-view image. (c) Cross-sectional profile along the line in image (b).

roughnesses were 3.3 and 3.4 nm, respectively (Figures 6 and 7). Typical nanodomains in both images had a half-height diameter of 23 nm and a height of 12 nm. With the molecular weight of PS increasing to 23 700, the surface roughness reached the maximum, 3.5 nm (sample **10**). The size and the height of a typical domain were ∼30 nm and ∼11 nm, respectively (Figure 8). With the increase of the molecular weight of PS to a value higher than that of PMMA, the surface roughness decreased to 1.9 nm (sample **11**, Figure 9). While the size of the typical domain was bigger (∼35 nm), the height was smaller (∼7 nm). Further increasing the molecular weight of PS relative to that of PMMA, both the surface roughness (1.2 nm in Figure 10 for sample **12** and 0.8 nm in Figure 11 for sample **13**) and the variations of the surface features diminished. A transition in the shape of nanodomains was observed from the top-view AFM images (2-D images). The variation of the surface feature in sample **7** was small and random. Individual nanoscale domains were clearly observed in samples **8** and **9** (Figures 6b and 7b). From sample **10** to **12**, the domains became connected, and the variation in the height of the domains gradually decreased (Figures 8b, 9b, and 10b). Eventually, the domains were well-connected with each other and evolved into random variations with no individual domains (Figure 11b, sample **13**). The best images were observed when the PS molecular weight was slightly lower than that of PMMA, and the highest contact angle was observed when the PS molecular weight was slightly higher than that of PMMA. It should be pointed out that the changes in the surface morphologies and water contact angles are reversible. After treatment with chloroform again, the surfaces exhibited essentially the same water contact angles as after first treatment with chloroform (Table 2).[46]

We speculate that the nanoscale domains appearing in Figures 6−8 are of micellar structures (Scheme 4). For the sample with

(46) AFM images of samples **9** and **11** after chloroform treatment can be found in the Supporting Information. The surfaces were smooth with surface roughnesses of 0.51 nm (sample **9**) and 0.53 nm (sample **11**).

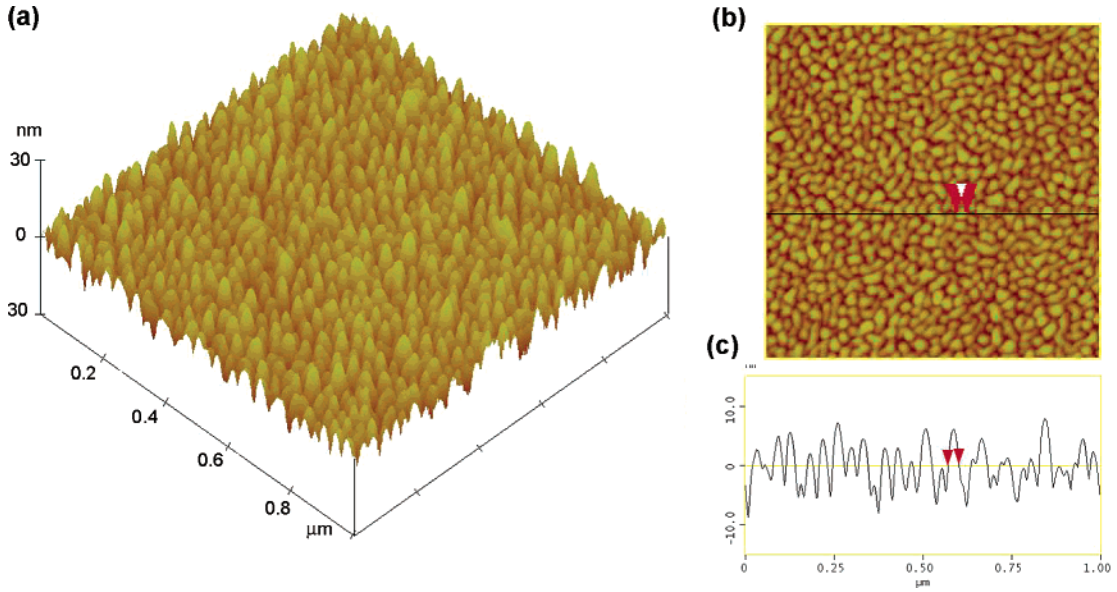

Figure 8. AFM images of sample **10** after treatment with glacial acetic acid. (a) 3-D image. (b) 2-D top-view image. (c) Cross-sectional profile along the line in image (b).

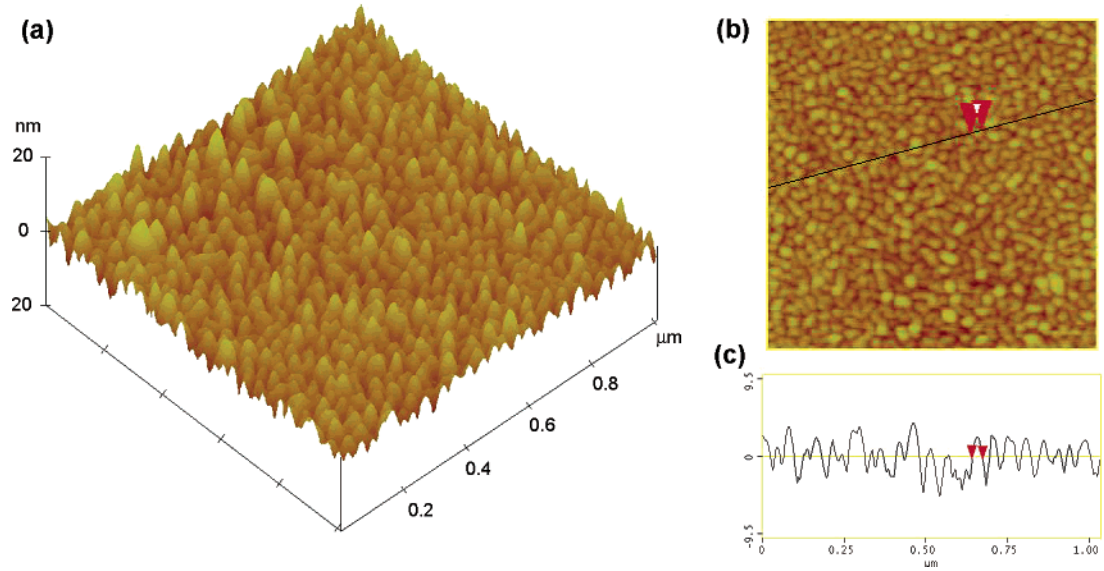

Figure 9. AFM images of sample **11** after treatment with glacial acetic acid. (a) 3-D image. (b) 2-D top-view image. (c) Cross-sectional profile along the line in image (b).

very short PS chains (e.g., in sample **7**), PMMA chains dominated the outermost layer as in a pure PMMA brush and consequently exhibited a surface composed of random features with a small variation in height after treatment with AA. For samples **8**−**10**, the values of water θ_a were between 74° and 91° after treatment with chloroform, indicating that both PS and PMMA chains were present in the water sensing region. Treatment with AA made PS chains collapse and aggregate with each other to minimize the contacts with acetic acid. On the other hand, the PMMA chains formed a diffusive layer around the PS cores and shielded the PS chains from the solvent (the "flowerlike" structure as discussed by Singh et al.[25]). Washing with water made PMMA chains collapse and form a shell around the PS core. This speculation was supported by XPS studies that showed that PMMA was enriched in the outermost layer. With the PS M_n increasing to a value significantly higher than that of PMMA, reorganization becomes difficult for both polymer chains, making the micellar structures ill-defined, and eventually the relatively ordered structures evolved into a random surface.

It can be envisioned that many factors can affect the formation of surface-tethered micelles. These factors include the Flory−Huggins interaction parameters between the two polymers and between each polymer and the solvent, molecular weight of each polymer chain, the overall grafting density, and the grafting density of each polymer. In this work, we investigated the effect of the molecular weight. Distinct surface morphologies after treatments with cyclohexane and AA observed in the present studies might result from the differences in polymer−solvent interactions. AA is a much better solvent for PMMA than cyclohexane for PS. We are attempting to elucidate the structures of nanodomains, seeking better-ordered patterns, and exploring the effects of other parameters.

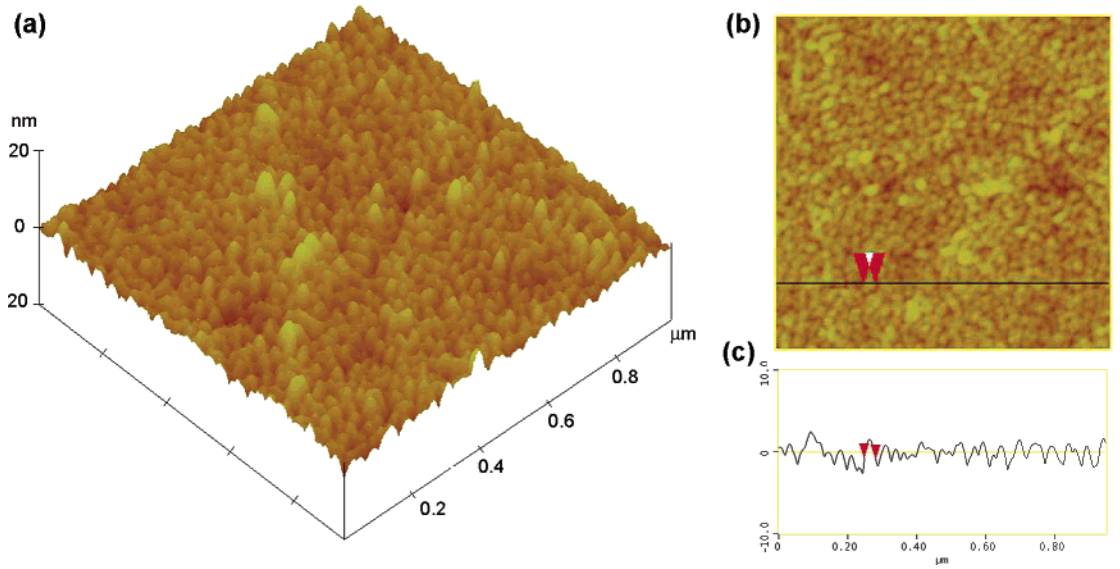

Figure 10. AFM images of sample **12** after treatment with glacial acetic acid. (a) 3-D image. (b) 2-D top-view image. (c) Cross-sectional profile along the line in image (b).

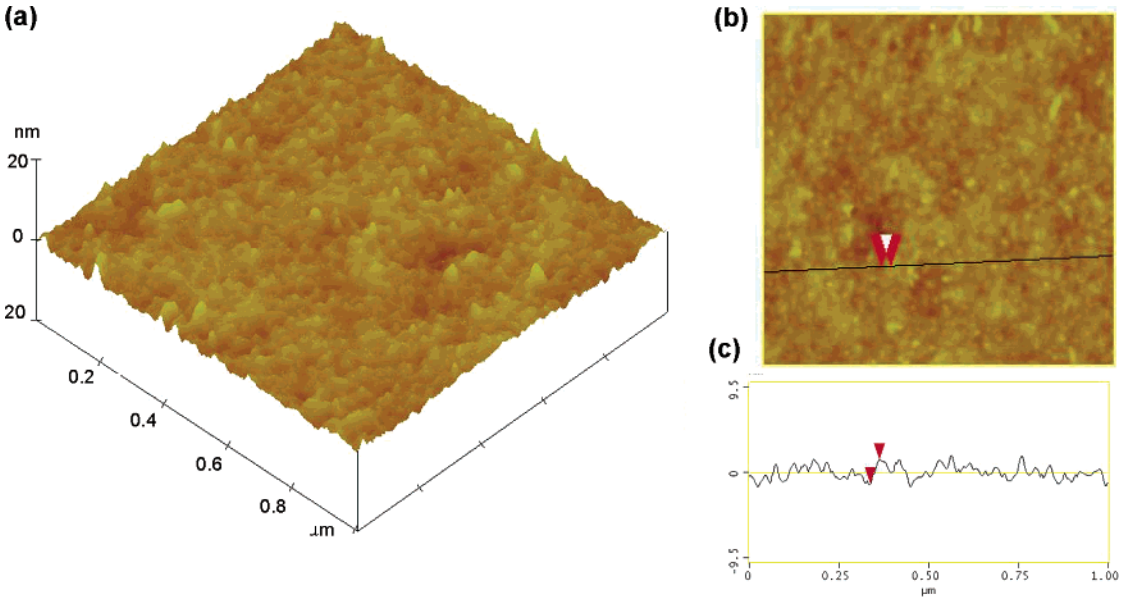

Figure 11. AFM images of sample **13** after treatment with glacial acetic acid. (a) 3-D image. (b) 2-D top-view image. (c) Cross-sectional profile along the line in image (b).

Scheme 4. Schematic Illustration of the Surface Micelles Formed from Mixed PMMA/PS Brushes Induced by Treatment with Glacial Acetic Acid

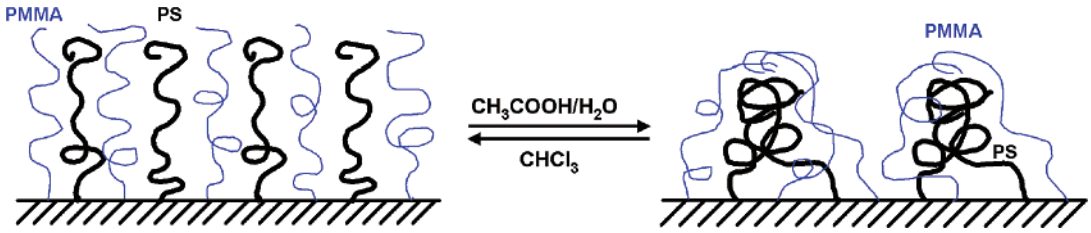

Conclusion

Mixed PMMA/PS brushes with various molecular weights after treatments with different solvents were characterized by contact angle measurements, XPS, and AFM. For a series of mixed brushes with a fixed PMMA M_n and systematically changed PS M_n, a transition in water θ_a from 74° to 91° was observed after treatment with $CHCl_3$ with the increase of the PS M_n. AFM studies showed that the surfaces were smooth. It was observed that the mixed brushes with PS M_n slightly smaller than that of PMMA underwent self-reorganization in cyclohexane and exhibited different surface wettabilities. However, no significant changes in surface morphologies were found. Relatively ordered nanoscale domains were observed in the mixed brushes with PS M_n slightly lower than or similar to that

of PMMA after treatment with glacial acetic acid, a selective solvent for PMMA. XPS studies confirmed that the PMMA chains were enriched at the outermost layer. It is speculated that the nanodomains are of micellar structures, with PS forming the core and PMMA chains forming the shell around the PS core. Further experimental study of the structure of the nanodomains is needed and underway.

Acknowledgment. B.Z. thanks the University of Tennessee at Knoxville (start-up funds) and the American Chemical Society Petroleum Research Funds (PRF No. 40084-G7) for supporting this research. AFM and XPS studies were carried out in the Center for Microanalysis of Materials at the University of Illinois at Urbana-Champaign, which is partially supported by the U.S. Department of Energy under Grant DEFG-02-91-ER45439.

Supporting Information Available: Experimental section, including materials, characterization, treatment with cyclohexane and glacial acetic acid, AFM images of samples **9** and **11** after treatment with chloroform (PDF). This material is available free of charge via the Internet at http://pubs.acs.org.

JA049570F